Geobiology (2009), 7, 25–34 DOI: 10.1111/j.1472-4669.2008.00186.x

Degeneration of biogenic superparamagnetic magnetite

Y.-L. LI,[1] S. M. PFIFFNER,[2] M. D. DYAR,[3] H. VALI,[4] K. KONHAUSER,[5] D.R. COLE,[6] A. J. RONDINONE[6] AND T. J. PHELPS[7]

[1]*Department of Earth Sciences and School of Biological Sciences, The University of Hong Kong, Hong Kong*
[2]*Center for Environmental Biotechnology, The University of Tennessee, Knoxville, TN 37966, USA*
[3]*Department of Astronomy, Mount Holyoke College, 50 College Street, South Hadley, MA 01075, USA*
[4]*Department of Earth and Planetary Sciences, 3640 University Street, McGill University, Montreal, Quebec H3A 2B2, Canada*
[5]*Department of Earth and Atmospheric Sciences, University of Alberta, Edmonton, Alberta, T6G2E3, Canada*
[6]*Chemical Sciences Division, Oak Ridge National Laboratory, Oak Ridge, TN 37831, USA*
[7]*Biological Science Division, Oak Ridge National Laboratory, Oak Ridge, TN 37831, USA*

ABSTRACT

Magnetite crystals precipitated as a consequence of Fe(III) reduction by *Shewanella algae* BrY after 265 h incubation and 5-year anaerobic storage were investigated with transmission electron microscopy, Mössbauer spectroscopy and X-ray diffraction. The magnetite crystals were typically superparamagnetic with an approximate size of 13 nm. The lattice constants of the 265 h and 5-year crystals are 8.4164Å and 8.3774Å, respectively. The Mössbauer spectra indicated that the 265 h magnetite had excess Fe(II) in its crystal-chemistry ($Fe^{3+}_{1.990}Fe^{2+}_{1.015}O_4$) but the 5-year magnetite was Fe(II)-deficient in stoichiometry ($Fe^{3+}_{2.388}Fe^{2+}_{0.419}O_4$). Such crystal-chemical changes may be indicative of the degeneration of superparamagnetic magnetite through the aqueous oxidization of Fe(II) anaerobically, and the concomitant oxidation of the organic phases (fatty acid methyl esters) that were present during the initial formation of the magnetite. The observation of a corona structure on the aged magnetite corroborates the anaerobic oxidation of Fe(II) on the outer layers of magnetite crystals. These results suggest that there may be a possible link between the enzymatic activity of the bacteria and the stability of Fe(II)-excess magnetite, which may help explain why stable nano-magnetite grains are seldom preserved in natural environments.

Received 28 August 2008; accepted 10 December 2008

Corresponding author: Y.-L. Li. Tel.: (852) 28598021; fax: (852) 25176912; e-mail: yiliang@hku.hk

INTRODUCTION

Magnetite can be classified as superparamagnetic (SP), single domain (SD) or multidomain (MD) according to both size and shape-constrained magnetic anisotropies. Many Fe(III)-reducing bacteria (IRB), including the genera of Geobacteraceae, *Shewanella* and *Thermoanaerobacter*, are capable of facilitating the extracellular precipitation of magnetite through their production of dissolved Fe(II) [reaction 1], and its subsequent abiological reaction with ferric iron [reaction 2]:

$$[1] \quad CH_3COO^- + 8Fe(OH)_3 \rightarrow 8Fe^{2+} + 2HCO_3^- + 15OH^- + 5H_2O$$

$$[2] \quad 2OH^- + Fe^{2+} + 2Fe(OH)_3 \rightarrow Fe_3O_4 + 4H_2O$$

The resulting magnetite crystals average less than 20 nm in diameter (Lovley *et al.*, 1987; Moskowitz *et al.*, 1989; Lovley, 1990; Sparks *et al.*, 1990; Moskowitz *et al.*, 1993; Hanzlik *et al.*, 1996; Zachara *et al.*, 2002; Roh *et al.*, 2003; Kukkadapu *et al.*, 2005; Stapleton *et al.*, 2005; Roh *et al.*, 2006), which places them within the size range of SP magnetite (Dunlop & Özdemir, 1997). The extracellularly precipitated magnetite in IRB cultures is also generally irregular in morphology (e.g. Frankel and Bazylinski, 2003), as compared to the rectangular, cubic or arrow-shaped forms generated by the magnetotactic bacteria, which form intracellular chains of SD magnetite (Bazylinski and Moskowitz, 1997).

Interestingly, Frankel (1987) and Lovley (1990) estimated that magnetite produced by IRB could be several thousand times more than magnetotactic bacteria do per unit of biomass,

suggesting that 'biologically induced' magnetite may play a prominent biological role in the natural environment. However, in natural sediments, there have been few reports demonstrating the unequivocal existence of extracellularly precipitated magnetite (e.g. Gibbs-Eggar *et al.*, 1999; Maloof *et al.*, 2007) compared to studies showing chains of magnetosomes from magnetotactic bacteria (e.g. Frankel *et al.*, 1979; Kim *et al.*, 2005; Pan *et al.*, 2005; Housen & Moskowitz, 2006; Kopp & Kirschvink, 2008). This discrepancy might be caused by the possibility that nanometer-size SP magnetite is less stable than the larger SD particles (Tarduno, 1995). For instance, the typical nano-material (with a particle size around 10 nm) has about 25% of its atoms on the surface layers, whereas SD magnetite from magnetotactic bacteria (with a size of approximately 80 nm) may have <2.5% of the atoms on the particle surfaces (Navrotsky, 2000). Therefore, the SP magnetite has thousands of times higher surface energy than bulk magnetite, and consequently, its surface provides an active substrate for physical, chemical and biological reactions (Navrotsky, 2000). As observed in the laboratory, cell growth leads to shifts in geochemical conditions, such as Eh, pH and higher Fe(II) concentrations (e.g. Bell *et al.*, 1987), that favour the mineralization of magnetite (e.g. Zhang *et al.*, 1998; Zachara *et al.*, 2002; Roh *et al.*, 2003). Accordingly, the cessation of cell growth should have consequences on the stability of magnetite because the last stages of biomineralization are inorganically driven (Konhauser, 1997), yet this aspect of magnetite stability is poorly resolved. Controversial explanations, such as reductive dissolution (e.g. Dong *et al.*, 2000; Kukkadapu *et al.*, 2005; Maloof *et al.*, 2007), abiotic dissolution by organic matter (e.g. Hilgenfeldt, 2000; Snowball, 1993), and aqueous oxidation (Hanzlik *et al.*, 1996; Tang *et al.*, 2003) were suggested to be responsible for the instability of biogenic SP magnetite.

In order to assess whether SP magnetite is indeed unstable, we compared the crystal-chemistry and lattice constant (LC) of magnetite produced by *Shewanella algae* strain BrY after 265 h incubation at 30 °C, and those after further storage under anaerobic conditions for ~5 more years at room temperature. We show through the use of wet chemistry, X-ray diffraction (XRD), transmission electron microscopy (TEM) and Mössbauer spectroscopy that SP magnetite crystals indeed undergo crystal-chemical modification with time, which might explain the paucity of biogenic SP magnetite reported from modern sediments and the rock record.

MATERIALS AND METHODS

Bacteria and wet-chemical analyses

Shewanella algae strain BrY (Caccavo *et al.*, 1992) and *Shewanella* strain PV4 were incubated with the basal medium prepared by adding 3-g NaH_2PO_4, 0.1-g KCl and 1.5-g NH_4Cl as the nutrients, 10-g sodium PIPES (Piperazine-N,N′-bis(2-ethanesulfonic acid) sesquisodium salt) as the organic buffer, 1 mL vitamin solution, 10 mL mineral solution (Phelps *et al.*, 1989) and 1 mL 0.5% rezasurin to 1 L deionized distilled water. The medium was then heated to 70 °C accompanied by spontaneous degassing by N_2, cooled to room temperature, dispensed at 10 mL into 26 mL pressure tubes under N_2 atmosphere, capped with butyl rubber stoppers and aluminum crimp seals and sterilized. Presence of oxygen in the tube was tested by the reagent rezasurin, which turns the colour of the medium to pink. The two-line ferrihydrite (FHO) (e.g. Kukkadapu *et al.*, 2003) was added to the medium with a concentration equivalent to 50 mM Fe(III) as electron acceptor, and 10 mM lactate was added as the sole electron donor. Fe(III)-NTA (nitrilotriacetic acid) solution was added to provide a 4-mM water-soluble Fe(III) to initiate the growth, and 2.5 mM $FeCl_2$ was added to the medium to further exhaust free oxygen. The pH before incubation was 7.2. BrY was inoculated at 10% volume and incubated at 30 °C. Tubes prepared with the same conditions without inoculation were used as controls and were sacrificed at the beginning of incubation and the end of experiments. *Thermoanaerobacter* strain C1, which shares similar physiology and behaviours of biomineralization with *Thermoanaerobacter sp.* strain TOR39 was incubated at 55 °C with conditions the same as in Zhang *et al.* (1998). Magnetite was extracted and treated with same methods as for BrY cultures.

Magnetite used for high-resolution TEM observation was collected from the incubation of *S. algae* BrY and *Shwanella* strain PV4. Subsamples for water soluble (WS)-Fe(II) and Fe(III), and 0.5 M HCl extractable Fe(II) and Fe(III) were measured using a SHIMADZU UV-VIS spectrophotometer with the procedures described in Li *et al.* (2006) and the method described in To *et al.* (1999). The extracted Fe(II) and Fe(III) were regarded as bioavailable iron. Triplicate tubes were used for checking time points. The tube that contained the biogenic magnetite was opened in the anaerobic chamber that contained 99% N_2 and 1% H_2. The solid phase was washed with O_2-free water several times and once with methanol, and placed in the anaerobic chamber for drying. The dried solid was stored in the 1.5 mL vial with 99% N_2 + 1% H_2 headspace gases for further analysis.

Mössbauer spectroscopy, TEM and XRD

Room temperature Mössbauer spectroscopy was conducted at the Institute for Rock Magnetism, University of Minnesota on the 265 h sample (M265h hereafter) and at Mount Holyoke College for a sample that was incubated for 5 more years at room temperature (M5Y hereafter). The sample was prepared by sealing about 10 mg of freeze-dried powder in a Teflon ring of 1 cm diameter by brown, low-temperature plastic tape. Spectra were recorded using a source of 50 mCi ^{57}Co diffused in the Rhodium film, moving in a constant acceleration mode with a symmetric double ramp wave form. Spectra were subsequently folded to eliminate the parabolic background before fitting. The velocity scale was calibrated with reference to the spectra of a α-Fe foil. Highly purified helium gas was

Table 1 The Mössbauer hyperfine parameters of the iron minerals in BrY cultures

Sample	δ mm s^{-1}	Δ mm s^{-1}	Hhf kOe	Area %	Assign.	Cation p.f.u.	L.C. Å
BrY (265 h)	0.28	−0.26	243	20	A-site	$Fe^{3+}[Fe^{3+}_{0.990}Fe^{2+}_{1.015}]O_4$	8.4164
	0.66	0.05	416	41	B-site		
	0.42			39	FHO		
BrY 5 Years	0.31	−0.27	236	47	A-site	$Fe^{3+}[Fe^{3+}_{1.388}Fe^{2+}_{0.419}]O_4$	8.3774
	0.35	−0.02	423	20	B-site		
	0.33	0.94		33	FHO		

δ: chemical shift; Δ: quadrupole splitting; Hhf: internal magnetic field. Assign: the assignments of cation occupations on A-site and B-site of magnetite and ferrihydrite (FHO). L.C.: lattice constant of magnetite.

flushed during the resonance absorption step. The spectra were fitted by using MO.exe (J.Y. Ping), which is suitable for simple spectra of ^{57}Fe.

At Mount Holyoke College, ~10 mg of sample was crushed under acetone, then mixed with a sugar-acetone solution designed to form sugar coatings around each grain in order to prevent preferred orientation of particles. Grains were gently placed in a sample holder confined by Kapton tape. Mössbauer spectra were acquired using a source of ~80 mCi ^{57}Co in Rh on a WEB Research Co. model WT302 spectrometer. Run time of 24 h resulted in 2 million baseline counts after the Compton correction. Spectra were collected in 2048 channels and corrected for nonlinearity via interpolation to a linear velocity scale, which is defined by the spectrum of the 25 μm Fe foil used for calibration. Data were then folded and processed using an in-house program from the University of Ghent, in Belgium called Mexfield.

Errors on isomer shifts were estimated at ±0.02 mm s^{-1}, and ±0.05 mm s^{-1} for quadrupole splitting. The error of area among multiple Fe^{2+} doublets/sextets or among multiple Fe^{3+} doublets/sextets was ±5–10%. The relative areas of iron fitted in different coordination sites have not been calibrated by the recoilless fraction. For example, the relative abundance of Fe at B-site to A-site is 2 for stoichiometric magnetite ($Fe^{3+}_A[Fe^{3+}Fe^{2+}]_BO_4$). If one considers that the recoilless fraction of B-site is smaller than that of A-site, the ratio of B-site to A-site of 1.88 fitted from Mössbauer spectroscopy is expected for standard stoichiometric magnetite (De Grave & Alboom, 1991). For the same reason, the relative abundances of the coexisting oxyhydroxides in M265h and M5Y should be slightly higher than those reported in Table 1 because of the presence of relatively small recoilless fraction of oxyhydroxides when compared to magnetite (De Grave & Alboom, 1991; Oh & Cook, 1999).

Morphological and structural changes of minerals were examined by TEM and XRD techniques. Conventional TEM analyses were conducted at the Microscopy Center of McGill University by methods as described previously (Vali *et al.*, 2004; Li *et al.*, 2006). High-resolution TEM imaging was conducted at the Center for Nanophase Materials Sciences of Oak Ridge National Laboratory. XRD measurements were conducted at the High Temperature Material Laboratory, Oak Ridge National Laboratory. The XRD samples were rinsed several times by N_2-purged water to remove salts that could contribute sharp unwanted peak in XRD patterns. The powder samples were scanned from 15 to 75°2θ values at 0.02° s^{-1}. The wavelength of Cu/K-α (1.54056Å) was used to calculate d-space values. Sample displacements off the diffractometer focusing circle were calibrated before doing Rietveld refinement. Lattice d-spacing values with ≥2σ errors were regarded as outliers and were rejected for LC calculation. Given its highly symmetrical structure, the Nelson-Riley extrapolation method (Nelson & Riley, 1945) was chosen to extrapolate LC to the 90° Bragg angle which eliminated the error propagated from the measurements of Bragg angles.

Reaction of fresh magnetite with fatty acid methyl esters

Dihydrocholestrol, hexadecanol, L-phenylalanine and a mixture of fatty acid methyl esters (FAME mixtures routinely used as standard for gas chromatography – mass spectrometer (GC-MS)) of C8–C24 with various structures were mixed with magnetite and incubated anaerobically at 37 °C and 70 °C to examine the potential for magnetite decomposition of environmentally relevant organics. Only the results of FAME mixtures were quantified. A mixture of fatty acid methyl esters 18–50 μg were mixed with ~5 mg dried magnetite in 24 mL pressure tubes under anaerobic condition. The tubes were previously sterilized at 450 °C for more than 6 h. The tubes were then capped with butyl rubber stopper, which had been washed with hexane and methanol and sealed with Al-crimps. The SD magnetite extracellularly produced by *Thermoanaerobacter* strain C1 at 55 °C was used as a control to assess the effect of particle size. The size of the SD magnetite was 64 ± 18 nm. The tubes were placed in incubators at the desired temperatures (37 °C and 70 °C) for 4 days. The FAMEs were extracted with the standard procedures as described previously (Li *et al.*, 2007) without the steps for esterification, followed by quantification and characterization by GC-MS at Center for Biomarker Analysis, University of Tennessee. The nomenclature of fatty acids can be found in Li *et al.* (2007). The solid relics were stored under anaerobic condition until examined by XRD and TEM examinations.

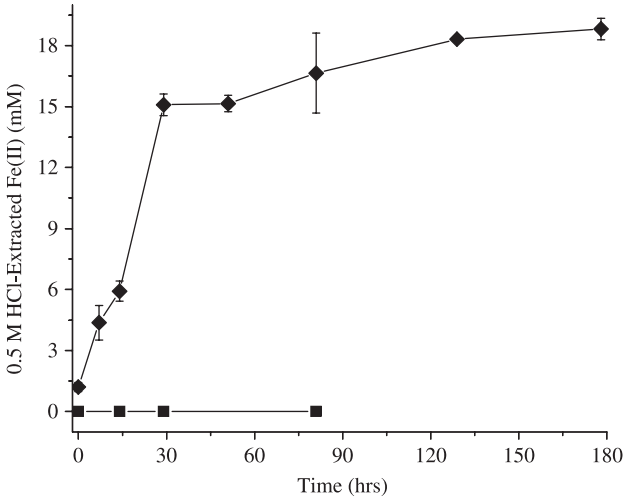

Fig. 1 Time course concentrations of 0.5 M HCl-extractable Fe(II) during the transformation of ferrihydrite to magnetite by *S. algae* BrY (diamond) and controls with same media but no inoculums added (square). Error bars represented the average of triple tubes.

RESULTS

Solution chemical changes

The 0.5 M HCl extracted Fe(II) during ferrihydrite transformation to magnetite showed significant increases in dissolved Fe(II) until approximately 29 h had elapsed (Fig. 1). Thereafter, the amount of Fe(II) increased only marginally. These changes in Fe(II) concentration correspond directly to changes in cell growth patterns, from exponential growth until approximately 29 h to stationary phase and through the remainder of the experiments (up to 178 h). No magnetite could be detected in the controls whose concentrations of Fe(II) showed little change throughout the course of the experiments. A parallel set of BrY culture showed 7.69 mM of WS-Fe(II) after 8 months incubation; whereas the WS-Fe(II) decreased sharply to 0.02 mM after more than 5 years of further incubation at room temperature. The extracted magnetite that showed no other minerals by XRD examination, yielded Fe(III)/Fe(II) ranges from 2.4 to 3.0 after being dissolved by 6 M HCl for wet-chemical analyses; whereas those with XRD-detectable siderite generally had Fe(III)/Fe(II) much less than 2.0.

Crystallite size and lattice parameters

The TEM images of M265h and M5Y under low magnification revealed agglomerations of magnetite with only slight differences in size and morphology (Fig. 2A,B). The particle sizes have been measured for 150 particles of M5Y yielding grain dimensions ranging from 6 to 26 nm, with an average of 12.9 ± 4.5 nm. The high-resolution TEM image of the magnetite reacted with fatty acids at 70 °C similarly showed minimal change in

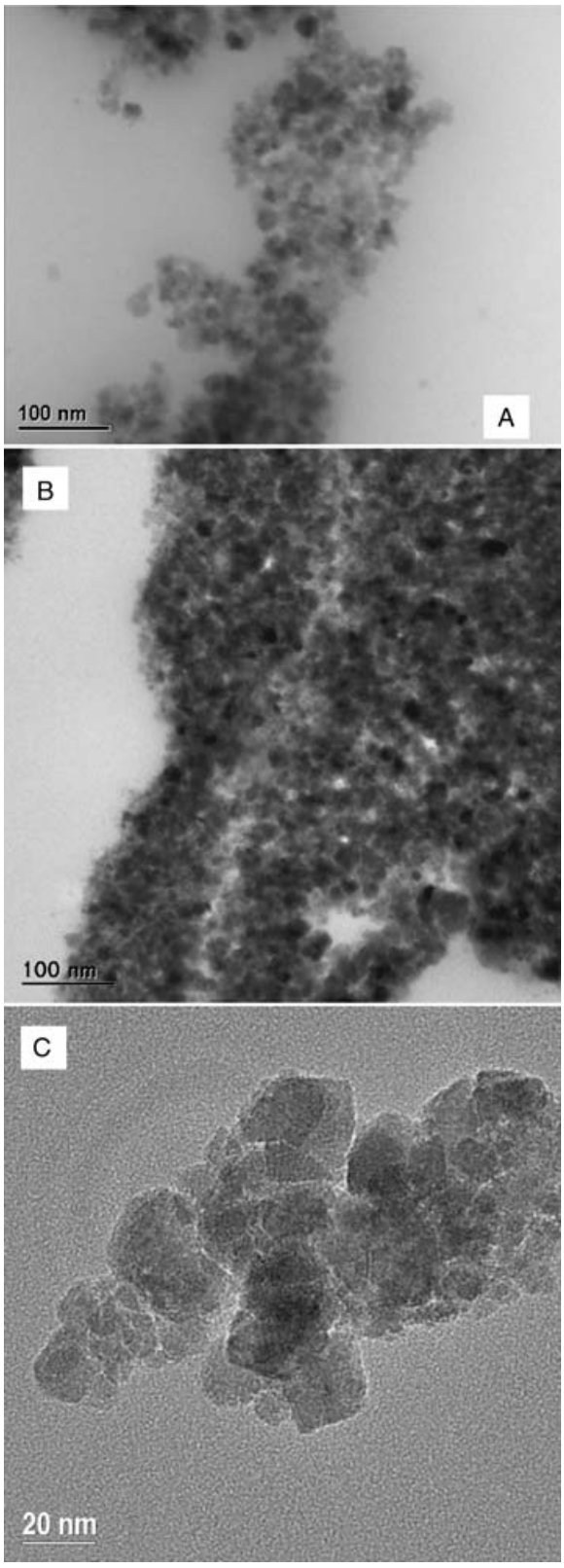

Fig. 2 TEM images of magnetite precipitated in BrY cultures. A: magnetite after 265 h incubation; B: magnetite after 5 more years incubation at room temperature; C: magnetite after reaction with fatty acids at 70 °C.

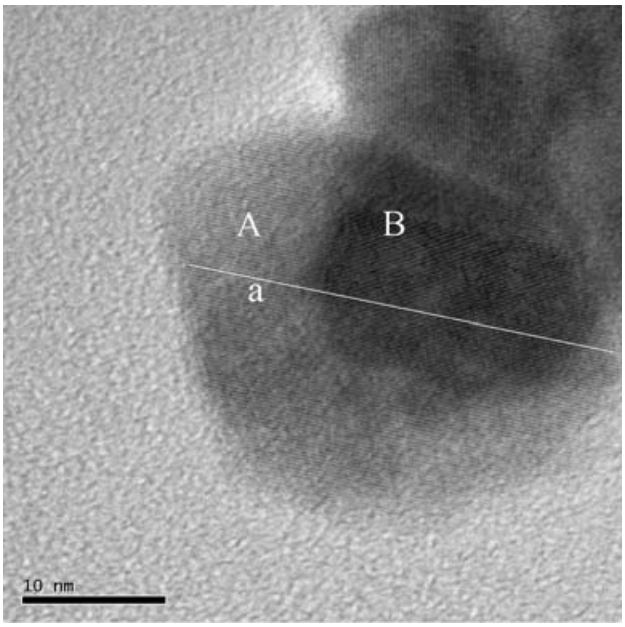

Fig. 3 The high-resolution TEM image of biogenic SP magnetite showed the corona structure (A) as the part experienced degeneration on the original magnetite crystals (B) as a result of the oxidization of Fe(II) in the lattice structure. Lattice fringes parallel to line 'a' passing both part A and part B indicated they were part of one single crystal.

morphology or particle size (Fig. 2C). In contrast, a high-resolution TEM of M5Y magnetite showed a corona structure (part A in Fig. 3) on the original magnetite (part B in Fig. 3). Importantly, the lattice fringes parallel to line 'a' passing through both A and B areas in Fig. 3 clearly demonstrated that they were two parts of one single crystal.

Because the magnetite is typically nano-sized, the corresponding XRD scans showed peak broadening in both M5Y and M265h (Fig. 4A,C). The LC calculated from Nelson-Riley extrapolation for M265h was 8.4164Å and for M5Y was 8.3774Å (Table 1). Good linearity indicated this method was successful (Fig. 4B,D). Reaction of magnetite crystals with dihydrocholesterol, hexadecanol, and L-phenylalanine resulted in significant shifts of their XRD peaks and accordingly a decrease of LC values. For example, after reacting with dihydrocholesterol at 70 °C magnetite had an LC of 8.3419Å; with L-phenylalanine at 70 and 37 °C had LC values of 8.3403 and 8.3665Å, respectively; these reacted with hexadecanol at 70 and 37 °C had LC values of 8.3609 and 8.3593Å, respectively. Comparatively, the magnetite synthesized at 70 °C has its LC of 8.3826Å, which slightly changed to 8.3766Å after reacting with dihydrocholesterol at 70 °C. Figure 2C shows a high resolution image of magnetite after reaction with fatty acids at 70 °C, which is consistent with the XRD and Mössbauer spectroscopic results indicating that no new phase appeared in the experiments.

Mössbauer spectroscopy and stoichiometry of M265h and M5Y

The Mössbauer spectroscopic profile data points of M265h and M5Y were plotted as error bars representing standard error (Dyar *et al.*, 2007). A paramagnetic phase, a magnetic sextet and a greatly broadened line of SP component for magnetite were fitted for both samples (M265h and M5Y in Fig. 5). The paramagnetic phase (with $\delta = 0.33$ and 0.42 mm s^{-1}, Table 1) could be assigned to an 'intermediate ferrihydrite' reported by Kukkadapu *et al.* (2003). The sextets with larger δ-values (0.66 and 0.35 mm s^{-1} for M265h and M5Y, respectively) were assigned to $Fe^{2.5+}$ in the B-site, and the broadened lines that gave smaller δ-values (0.28 and 0.31 mm s^{-1} for M265h and M5Y, respectively) were assigned to be the SP component for those spectra recorded at room temperature (Table 1). The Δ-values of B sites were close to those of bulk magnetite (e.g. De Grave *et al.*, 1993) whereas those of A sites ($-0.27 \sim -0.26$ mm s^{-1}) were significantly smaller than the bulk magnetite (~0.00 mm s^{-1}). Based on the ratio of B to A site from Mössbauer spectroscopy fitted areas, which is a sensitive measure of the stoichiometry (Daniels & Rosenswaig, 1969), the cations per formula units (p.f.u.) of M265h and M5Y were calculated to test for their departures from stoichiometry (Peev, 1995; Voogt *et al.*, 1999) (Table 1). The ferrihydrite doublets accounted for 33% of total iron in M5Y (Table 1), which is fairly constant with the percentage of amorphous component of M5Y calculated by XRD profiling ($36 \pm 3\%$).

Decomposition of complex organics by fresh biogenic magnetite

The FAME mixture incubated with magnetite included saturated, monounsaturated, polyunsaturated, branched fatty acids of either *trans*- or *iso*-geometries with carbon numbers from 8–24 (Fig. 6B). At 70 °C, the FAMEs were totally decomposed after reaction with fresh SP magnetite with no FAME peak detected by GC-MS. For FAME mixture reacted with SP magnetite at 37 °C, 15 of 45 FAMEs survived the reaction whereas all those having carbon numbers less than 17 disappeared (Fig. 6A). As a comparison, FAME mixture reacted at 37 °C with SD magnetite produced extracellularly by C1 at 55 °C had 26 FAMEs survived with all those having carbon numbers less than 14 disappeared (Fig. 6C). The relative abundances of fatty acids with different carbon numbers and varied structures changed as a result of their heterogeneous reactivities to magnetite. For example, fatty acid 18 : 1ω9c was 1.27% in the fresh mixture, which increased to 20.34% after reacting with SD magnetite and became 15.44% after reacting with SP magnetite at 37 °C; fatty acid 22 : 0 was 6.69% in the fresh mixture, increased to 15.12% after reacting with the SD magnetite and became 24.44% after reacting with SP magnetite at 37 °C. Fatty acid

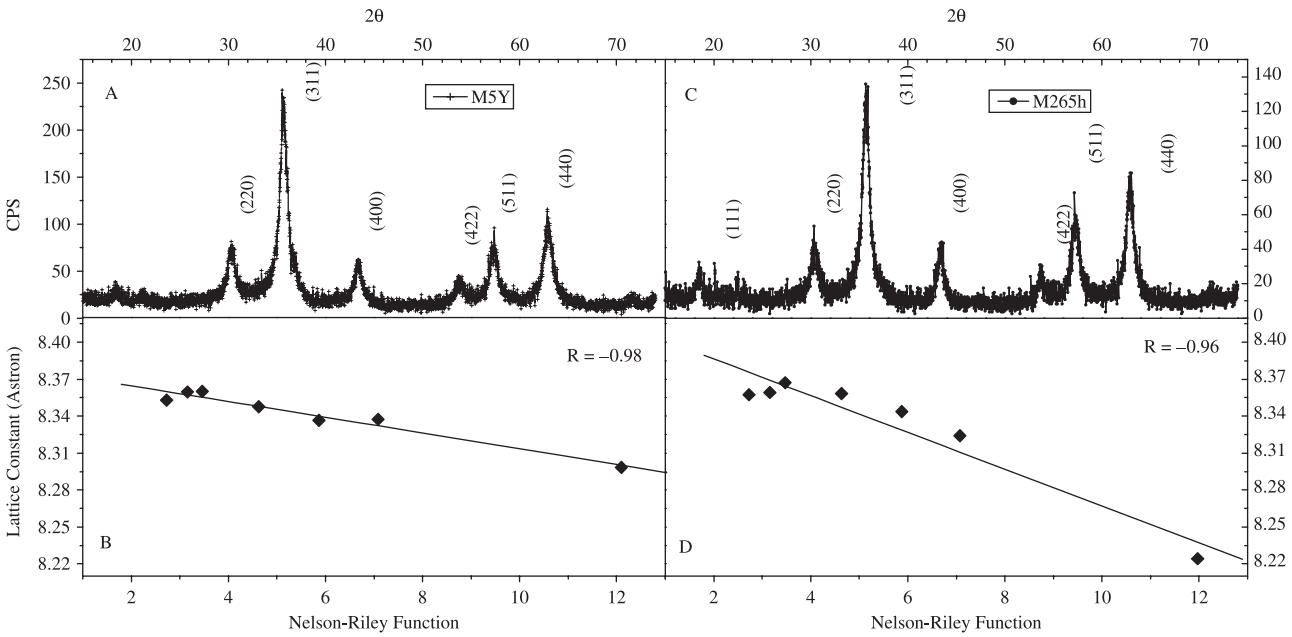

Fig. 4 XRD patterns of M5Y (A) and M265h (C) and the Nelson-Riley functions used to extrapolate the lattice constants at 90° Bragg angles for M5Y (B) and M265h (D). The XRD pattern showed no new mineral in the aged culture.

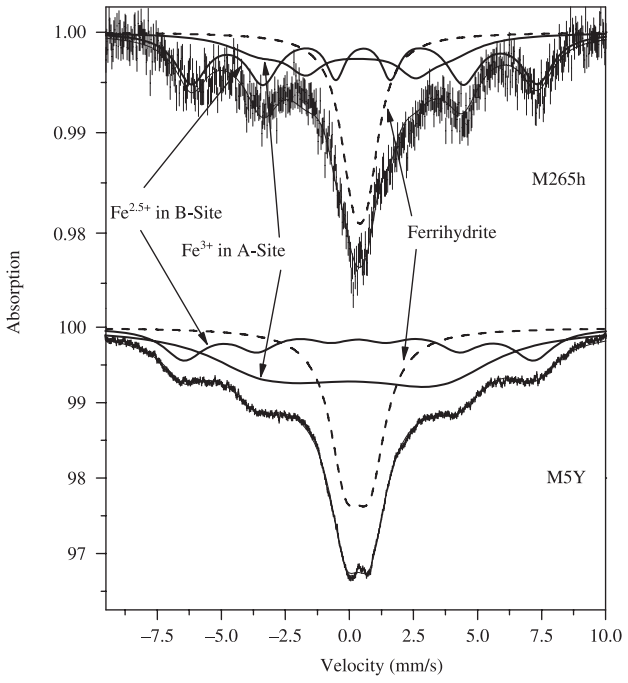

Fig. 5 Room temperature Mössbauer spectra of magnetite precipitated in BrY cultures after 265 h (M265h) and 5 years (M5Y) storage anaerobically.

17 : 0 was 1.41% in the fresh mixture, which decreased to 0.88% in the SD magnetite and was under the detection limit after reacting with SP magnetite at 37 °C. Some fatty acids, such as 18 : 0, 10Me18 : 0 just changed slightly in their percentage compositions after reacting with SP- and SD magnetite crystals at 37 °C.

DISCUSSION

Incomplete mineral transformation induced by bacterial iron reduction

Although powder XRD patterns showed magnetite to be the only crystalline phase in both M265h and M5Y for BrY experiments (Fig. 4A,C), the Mössbauer spectroscopic structures indicated an incomplete transformation of the precursor ferrihydrite to magnetite (Fig. 5). The amorphous component observed for M265h accounted for 36% of the total area of the XRD profile, a result that correlated well with Mössbauer spectroscopy, which yielded 39% FHO for M265h (Table 1). Mössbauer measurements of extracellular magnetite in the other IRB cultures also indicated the presence of a non-magnetite Fe(III)-precursor phase at the end of the experiments (3.4–10.3%). Wet-chemical analysis of extracted biogenic magnetite precipitated by *S. algae* strain BrY and *Thermoanaerobacter* TOR39 yielded Fe(III)/Fe(II) as high as 2.3 and 2.4, respectively. Similarly, wet-chemical analyses of Fe(II)/Fe(III) ratios in magnetite produced by the other IRB, such as *Shewanella putrefaciens* strain CN32 and *Geobacter metallireducens* strain GS-15 also demonstrated significant deviations from magnetite stoichiometry. It is obvious that the chemistry of aqueous part and the solid part still evolves after the cessation of biological activity.

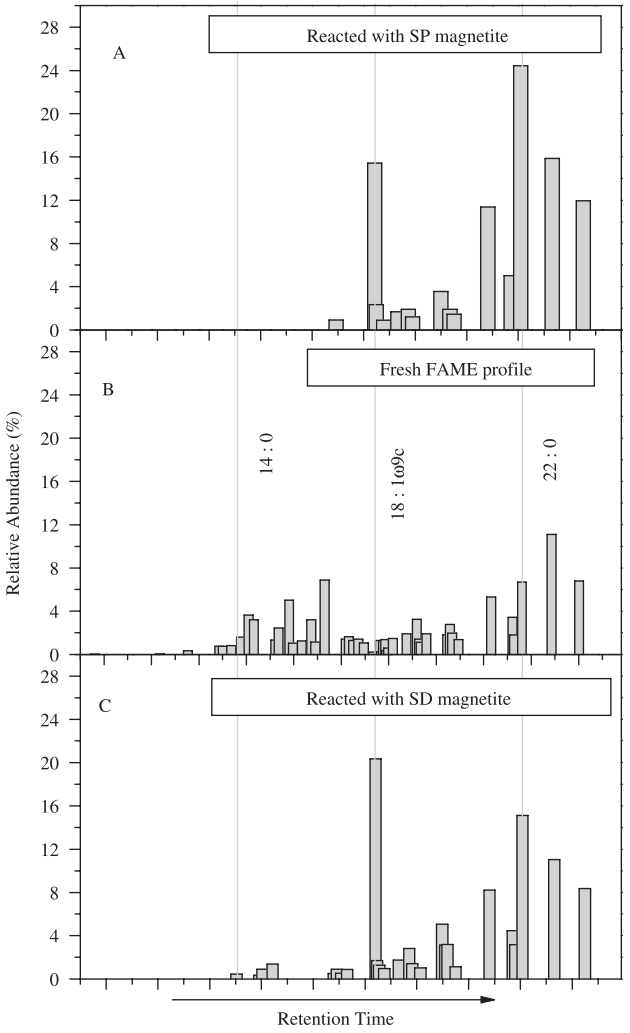

Fig. 6 Profiles of FAME mixture after reacted with biogenic magnetite crystals anaerobically. (A) FAMEs reacted at 37 °C with SP magnetite produced by BrY; (B) the profile of original FAME mixture; (C) FAMEs reacted at 37 °C with SD magnetite produced by *Thermoanaerobacter* strain C1.

The degeneration of Fe(II)-excess magnetite to Fe(II) depleted composition

The iron ratio of B to A site from Mössbauer spectroscopy is a sensitive indicator of the Fe(III)/Fe(II) ratio and stoichiometric composition of magnetite (e.g. McCammon *et al.*, 1986; Aragón, 1992; Voogt *et al.*, 1999; Zhang *et al.*, 2000). The ratio of the relative areas of B to A for M265h is larger than the 2.00 (after recoilless fraction calibration) of stoichiometric magnetite, indicative of excess Fe(II) (1.015 p.f.u Fe(II)) in its structure (Table 1), and in agreement with crystal-chemical compositions of magnetite precipitated in *Shewanella* cultures (Kukkadapu *et al.*, 2005; Hanzlik *et al.*, 1996). However, the B to A ratio of M5Y was significantly lower than 2.00 (Table 1), which implies Fe(II) depletion in the B-site (Fe(II) = 0.419 p.f.u.) without any transformation in mineralogy, as also indicated by XRD patterns (Fig. 4A,C).

The LC of M265h is larger than that of the theoretical value for standard stoichiometric magnetite (8.3967Å of Fe_3O_4, Zhang & Saptathy, 1991) because of the incorporation of excess Fe(II) cation with a large Goldschmidt radius (0.92Å) in the octahedral coordinated site; conversely, the LC of M5Y is smaller than the stoichiometric magnetite because of the replacement of Fe(II) cation by Fe(III) cation with a small radius (0.785Å) in the octahedral coordinated site (Shannon, 1976). The shift of crystal-chemical composition of magnetite was corroborated by high-resolution TEM observation of aged magnetite produced by BrY and the *Shewanella* strain PV4, which shares the same physiology and behaviour of magnetization (Fig. 3). The corona (A area in Fig. 3) represents a portion of magnetite with a modified Fe(II)/Fe(III) composition. The corona (A area) and the major part (B area) were obviously two parts of one single crystal because they share continuous set of lattice fringes parallel to line a (Fig. 3). The presentation of two sextets of Mössbauer hyperfine parameters (Table 1 and Fig. 5) indicated the magnetic-ordered phase is still magnetite. Moreover, the TEM results did not support the formation of new FeOOH species, which typically exhibit acicular-like morphologies.

It is indicated that after 5 years storage, the magnetic components increased about 6% (Table 1). The increase could be the result of the continuing magnetization of ferrihydrite through a nucleation mechanism (reaction 2), which is thermodynamically favoured because of the high concentration of soluble Fe(II), neutral or higher pH and activated ferric iron oxyhydroxide. The oxyhydroxide in M5Y had high Δ-value (0.94 mm s^{-1}), indicating a highly distorted Fe(III)-O octahedral micro-environments resulting from the soluble Fe(II) aided dissolution of ferrihydrite.

An interesting observation of this study is that the degeneration of this magnetite could be coupled with the decomposition of organic compounds (Fig. 6). Structural Fe(II) in synthetic magnetite treated with H_2 at elevated temperatures (McCammon *et al.*, 1986; Tamaura & Tabata, 1990; Zhang *et al.*, 2000) has been demonstrated to be a strong reductant. In this study, the decrease of LC (8.4164Å to 8.3419–8.3609Å) after reacting with magnetite similarly suggests that some of the FAME components may serve to oxidize the Fe(II) component in magnetite. The degeneration of Fe(II)-excess magnetite could be the hydrolysis of Fe(II) on the lattice of magnetite following a nucleation of those magnetite, as indicated in reaction 2. The Fe(II)-excess magnetite ($Fe^{3+}[Fe^{3+}Fe^{2+}_{1+\delta1}]O_4$) can be rewritten as $[Fe_2O_3{\cdot}(FeO)_{1-\delta2}]{\cdot}(FeO)_{\delta1+\delta2}$ ($0 < \delta1$ and $\delta2 < 1$). δ1 represents Fe(II) cations more than stoichiometric Fe_3O_4 does, and δ2 means a little more Fe(II) will be further oxidized to reach a stable composition ($Fe_{3-\delta2}O_4$). The excess FeO in magnetite is a strong reducing agent (e.g. Tamaura and Tabata 1990; Zhang *et al.*, 2000) that is able to reduce carboxylic acids leading to the formation of alcohols:

$$[3] \quad 6FeO + CH_3(CH_2)_nCOOH + H_2O \rightarrow 2Fe_3O_4 + CH_3(CH_2)_{n+1}OH$$

$n = 0, 1, 2$ and so on. This is an abiotic, anaerobic oxidation mechanism that transforms the Fe(II)-rich surface spheres of SP magnetite into compositionally stable magnetite by getting oxygen from water and/or organic molecules. The production of alcohols has been observed in cultures of thermophilic IRB (e.g. Wiegel & Ljungdahl, 1981; Wagner & Wiegel, 2008); whereas the shift of Fe(III)/Fe(II) composition of magnetite may be supported by observation of the low-temperature transformation of bacterial magnetite to maghemite below the iron redox boundary in pelagic sediments from the western equatorial Pacific (Smirnov & Tarduno, 2000). Based on the thermodynamic data in Amend & Shock (2001), the formation of magnetite rather than FeOOH species in reaction 3 is a thermodynamically favoured process. This assumption is supported by the lack of FeOOH species on the surface of magnetite crystals as indicated by XRD and TEM observations. Reactions 2 and 3 indicated an inevitable oxidation of biogenic Fe(II)-excess magnetite even under strictly anaerobic conditions.

Stability limit of Fe(II)-excess SP magnetite

The Fe(II)-excess characteristics of the biogenic SP magnetite is clearly distinguishable from magnetite crystals produced inorganically because microbial reduction of Fe(III) can maintain a high-soluble Fe(II)/Fe(III) ratio in cultures (~30 folds by BrY and ~100 folds by TOR39) at neutral to high pH conditions. We suggest that the cessation of microbial activity may, in part, be responsible for the degeneration of Fe(II)-excess magnetite. High concentrations of dissolved Fe(II) in neutral and higher pH solutions are unstable, undergoing oxidation to Fe(III) and subsequent hydrolysis (e.g. Kim *et al.*, 2003; Roh *et al.*, 2003). During the growth of microbes, Fe(III) is reduced to Fe(II), and both soluble and structural Fe(II) can be stabilized by the maintenance of favourable Eh conditions and reductive enzymes created by cell growth. After the cessation of microbial growth, the cell and exopolymers undergo decomposition, and the microenvironment may become less stable for dissolved Fe(II) as well as Fe(II) in the lattice of SP magnetite. Because magnetite is the end product of bacterial reduction of ferrihydrite (e.g. Lovley, 1990; Fredrickson *et al.*, 1998; Lloyd *et al.*, 2000), the further reduction of biogenic magnetite (Kostka & Nealson, 1995; Dong *et al.*, 2000; Kukkadapu *et al.*, 2005) should not happen to the newly precipitated crystals under the not-yet changed condition. The aqueous oxidation of Fe-excess magnetite results in a Fe(III)-rich, more chemically stable magnetite in non-sulfuric environments at neutral or higher pH (Canfield *et al.*, 1992). Therefore, the observed dissolution of biogenic magnetite (Tarduno, 1995; Hilgenfeldt, 2000; Snowball, 1993) might be a consequence of several combined biological and geochemical processes. For example, under neutral or higher pH conditions, the biogenic SP magnetite might be oxidized to a composition with low Fe(II) in the structure (this study) or even to maghemite (Smirnov & Tarduno, 2000), which would be bioavailable again for IRB and could be biologically reduced (e.g. Dong *et al.*, 2000) and reprecipitated to siderite (e.g. Kukkadapu *et al.*, 2005).

According to Sarda *et al.* (1987) and Antony *et al.* (2006), the specific surface area of 13 nm magnetite grains might be as high as 75 $m^2\ g^{-1}$, but the surface area decreases to about 12 $m^2\ g^{-1}$ when the grain size is around 80 nm. The SD magnetite precipitated in *Thermoanaerobacter* sp. (TOR39 and C1) cultures at thermophilic temperatures (Zhang *et al.*, 1998) and those precipitated by magnetotactic bacteria have larger particle sizes (*c.* 50 nm to 120 nm) (e.g. Bazylinski & Moskowitz, 1997; Kim *et al.*, 2005; Pan *et al.*, 2005) that have much lower specific surface areas and surface energies and hence are lower in chemical reactivity. In natural sediment, SD size magnetite crystals produced by magnetotactic bacteria dominate the biogenic magnetic particles in sediments, which can even be preserved for long geological time (e.g. Chang & Kirschvink, 1989; Kopp & Kirschvink, 2008). Consideration of its instability, the SP magnetite might finally be transformed to siderite without the coexistence of magnetite (Mortimer *et al.*, 1997; Sawiki & Brown, 1998).

CONCLUSIONS

The magnetite precipitated by the metabolism of iron-reducing bacteria at mesophilic or psychrophilic temperatures is a typical nano-material that is characterized by its *c.* 13 nm particle size with superparamagnetic behaviour and high chemical activity. The freshly precipitated magnetite has a characteristic Fe(II)-excess stoichiometry and a larger LC than that of stoichiometic magnetite. After years of storage at room temperature, the composition degenerates to a Fe(II)-deficient crystal-chemistry with a smaller LC. This variation results from the aqueous oxidation of Fe(II) in the solution and Fe(II) in the lattice of magnetite. Oxidization of biogenic SP magnetite is evidenced by the high-resolution TEM observation of the corona structure on the original magnetite. This process follows the cessation of the bacterial activity, which can maintain a stable condition for Fe(II) at neutral and higher pH conditions. An oxidant for the Fe(II) component in magnetite could be various organic components that were present in the initial solutions that utilize the electrons from Fe(II). The Fe(III)-rich magnetite degenerated from a Fe(II)-rich composition under anaerobic condition is chemically stable but can be enzymatically reduced by iron-reducing bacteria. These findings may help explain why superparamagnetic magnetite is seldom preserved in the surface biosphere. The high activity of the biogenic superparamagnetic magnetite to organics suggests that it can serve as an electron donor for buried organic carbon, which ultimately provides another link in the Fe-C cycle.

ACKNOWLEDGEMENTS

This research was supported by NASA Astrobiology Institute grant to the Indiana-Princeton-Tennessee Astrobiology Initiative led by L.M. Pratt. Mössbauer spectroscopy at Mount Holyoke College was supported by NASA grant NNG04GG12G. Mössbauer spectroscopy at University of Minnesota was supported by the Institute for Rock Magnetism which is founded by the Keck Foundation, NSF, and the University of Minnesota. DRC was funded by the Division of Chemical Sciences, Geosciences and Energy Biosciences of the Office of Basic Energy Sciences, US Department of Energy under contract DE-AC05-00OR22725 to Oak Ridge National Laboratory, managed and operated by UT-Battelle, LLC. The manuscript was improved by the insightful comments from Dr Robert Kopp and an anonymous reviewer, and subject editor Lee Kump.

REFERENCES

Amend JP, Shock EL (2001) Energetics of overall metabolic reactions of thermophilic and hyperthermophilic Archaea and Bacteria. *FEMS Microbiology Review* **25**, 175–243.

Antony J, Nutting J, Baer DR, Meyer D, Sharma A, Qiang Y (2006) Size-dependent specific surface area of nanoporous film assembled by core-shell iron nanoclusters. *Journal of Nanomaterials* DOI: 10.1155/JNM/2006/54961, 1–4.

Aragón R (1992) Magnetization and exchange in nonstoichiometric magnetite. *Physical Review of B* **46**, 5328–5333.

Bazylinski DA, Moskowitz BM (1997) Microbial biomineralization of magnetic iron minerals: microbiology, magnetism and environmental significance. *Review in Mineralogy* **35**, 181–223.

Bell PE, Mills AL, Herman JS (1987) Biogeochemical conditions favoring magnetite formation during anaerobic iron reduction. *Applied and Environmental Microbiology* **53**, 2610–2616.

Caccavo F, Blakemore RP, Lovley DR (1992) A hydrogen-oxidizing, Fe(III)-reducing microorganism from the Great Bay Estuary, New Hampshire. *Applied and Environmental Microbiology* **58**, 3211–3216.

Canfield DE, Raiswell R, Bottrell S (1992) The reactivity of sedimentary iron minerals toward sulfide. *American Journal of Science* **292**, 659–683.

Chang S-BR, Kirschvink JL (1989) Magnetofossils, the magnetization of sediments, and the evolution of magnetite biomineralization. *Annual Review of Earth and Planetary Sciences* **17**, 169–195.

Daniels JM, Rosenswaig A (1969) Mössbauer spectroscopy of stoichiometric and non-stoichiometric magnetite. *Journal of Physics and Chemistry of Solids* **30**, 1561.

De Grave E, Van Alboom A (1991) Evaluation of ferrous and ferric Mössbauer fractions. *Physics and Chemistry of Minerals* **18**, 337–342.

De Grave E, Persoons RM, Vandenberghe RE, de Bakker PMA (1993) Mössbauer study of the high-temperature phase of co-substituted magnetites, $Co_xFe_{3-x}O_4$. I. $x \leq 0.04$. *Physical Review of B* **47**, 5881–5893.

Dong H, Fredrickson JK, Kennedy DW, Zachara JM, Kukkadapu RK, Onstott TC (2000) Mineral transformations associated with the microbial reduction of magnetite. *Chemical Geology* **169**, 299–318.

Dunlop DJ, Özdemir Ö (1997) *Rock Magnetism*. Cambridge University Press, 573 pp.

Dyar MD, Klima RL, Lindsley D, Pieters CM (2007) Effects of differential recoil-free fraction on ordering and site occupancies in Mossbauer spectroscopy of orthopyroxenes. *American Mineralogist* **92**, 424–428.

Frankel RB (1987) Anaerobes pumping iron. *Nature* **330**, 208.

Frankel RB, Bazylinski D (2003) Biologically induced mineralization by bacteria. *Review in Mineralogy and Geochemistry* **54**, 95–114.

Frankel RB, Blackmore RP, Wolfe R (1979) Magnetite in freshwater magnetotactic bacteria. *Science* **203**, 1355–1356.

Fredrickson JK, Zachara JM, Kennedy DW, Dong H, Onstott TC, Hinman NW, Li S (1998) Biogenic iron mineralization accompanying the dissimilatory reduction of hydrous ferric oxide by a groundwater bacterium. *Geochimica et Cosmochimica Acta* **62**, 3239–3257.

Gibbs-Eggar Z, Jude B, Dominik J, Loizeau J-L, Oldfield F (1999) Possible evidence for dissimilatory bacterial magnetite dominating the magnetic properties of recent lake sediments. *Earth and Planetary Science Letters* **168**, 1–6.

Hanzlik M, Petersen N, Keller R, Schmidbauer E (1996) Electron microscopy and ^{57}Fe Mössbauer spectra of 10 nm particles, intermediate in composition between Fe_3O_4 and γ-Fe_2O_3, produced by bacteria. *Geophysical Research Letters* **23**, 479–482.

Hilgenfeldt K (2000) Diagenetic dissolution of biogenic magnetite in surface sediments of the Benguela upwelling system. *International Journal of Earth Sciences* **88**, 630–640.

Housen BA, Moskowitz BM (2006) Depth distribution of magnetofossils in near-surface sediments from the Blake/Bahama Outer Ridge, western North Atlantic Ocean, determined by low-temperature magnetism. *Journal of Geophysical Research* **111**, G01005, doi: 10.1029/2005jg000068.

Kim BY, Kodama KP, Moeller RE (2005) Bacterial magnetite produced in water column dominates lake sediment mineral magnetism: Lake Ely, USA. *Geophysical Journal International* **163**, 26–37.

Kim DK, Mikhaylova M, Zhang Y, Muhammed M (2003) Protective coating of superparamagnetic iron oxide nanoparticles. *Chemistry of Materials* **15**, 1617–1627.

Konhauser KO (1997) Bacterial iron biomineralisation in nature. *FEMS Microbiology Reviews* **20**, 315–326.

Kopp RE, Kirschvink JL (2008) The identification and biogeochemical interpretation of fossil magnetotactic bacteria. *Earth-Science Reviews* **86**, 42–61.

Kostka JE, Nealson KH (1995) Dissolution and reduction of magnetite by bacteria. *Environmental Science and Technology* **29**, 2530–2540.

Kukkadapu RK, Zachara JM, Fredrickson JK, Smith SC, Dohnalkova AC, Russell CK (2003) Transformation of 2-line ferrihydrite to 6-line ferrihydrite under oxic and anoxic conditions. *American Mineralogist* **88**, 1903–1914.

Kukkadapu R, Zachara JM, Fredrickson JK, Kennedy DW, Dohnalkova AC, McCready DE (2005) Ferrous hydroxyl carbonate is a stable transformation product of biogenic magnetite. *American Mineralogist* **90**, 510–515.

Li YL, Vali H, Yang J, Phelps TJ, Zhang CL (2006) Reduction of iron oxides enhanced by a sulfate-reducing bacterium and biogenic H_2S production. *Geomicrobiology Journal* **23**, 103–117.

Li YL, Peacock AD, White DC, Geyer R, Zhang CL (2007) Spatial patterns of bacterial signature biomarkers in marine sediments of the Gulf of Mexico. *Chemical Geology* **238**, 168–179.

Lloyd JR, Sole VA, Van Praagh CVG, Lovley DR (2000) Direct and Fe(II)-mediated reduction of Technetium by Fe(III)-reducing bacteria. *Applied and Environmental Microbiology* **66**, 3743–3749.

Lovley DR (1990) Magnetite formation during microbial dissimilatory iron reduction. In *Iron Biominerals* (eds Frankel RB, Blakemore RP). Plenum Press, New York, pp. 151–166.

Lovley DR, Stolz JF, Nord GL, Phillips EJP (1987) Anaerobic production of magnetite by a dissimilatory iron-reducing microorganism. *Nature* **330**, 252–254.

Maloof AC, Kopp RE, Grotzinger JP, Fike DA, Bosak J, Vali H, Paussart PM, Weiss B, Kirschvink JL (2007) Sedimentary iron cycling and the origin and preservation of magnetization in platform carbonate muds, Andros Island, Bahamas. *Earth and Planetary Science Letters* **259**, 581–598.

McCammon CA, Morrish AH, Picone PJ, Pollard RJ, Sharrock MP (1986) Site occupancy and aging in hypermagnetite. *Journal of Magnetism and Magnetic Materials* **54–57**, 1695–1696.

Mortimer RJG, Coleman ML, Rae JE (1997) Effect of bacteria on the elemental composition of early diagenetic siderite: implications for palaeoenvironmental interpretations. *Sedimentology* **44**, 759–765.

Moskowitz BM, Frankel RB, Bazylinski DA, Jannasch HW, Lovley DR (1989) A comparison of magnetite particles produced anaerobically by magnetotactic and dissimilatory iron-reducing bacteria. *Geophysical Research Letters* **16**, 665–668.

Moskowitz BM, Frankel RB, Bazylinski DA (1993) Rock magnetic criteria for the detection of biogenic magnetite. *Earth and Planetary Science Letters* **120**, 283–300.

Navrotsky A (2000) Nanomaterials in the environment, agriculture, and technology (NEAT). *Journal of Nanoparticle Research* **2**, 321–323.

Nelson JB, Riley DP (1945) An experimental investigation of extrapolation methods in the derivation of accurate unit-cell dimensions of crystals. *Proceedings of the Physical Society* **57**, 160–177.

Oh SJ, Cook DC (1999) Mössbauer effect determination of relative recoilless fractions for iron oxides. *Journal of Applied Physics* **85**, 329–332.

Pan Y-X, Petersen N, Davila AF, Zhang L-M, Winklhofer M, Liu Q-S, Hanzlik M, Zhu RX (2005) The detection of bacterial magnetite in recent sediments of Lake Chiemsee (southern Germany). *Earth and Planetary Science Letters* **232**, 109–123.

Peev TM (1995) A Mössbauer study of synthetic magnetite. *Journal of Radioanalytical and Nuclear Chemistry* **199**, 289–294.

Phelps TJ, Raione EG, White DC, Fliermans CB (1989) Microbial activity in deep subsurface environments. *Geomicrobiology Journal* **7**, 79–91.

Roh Y, Zhang C-L, Vali H, Lauf RJ, Zhou J, Phelps TJ (2003) Biogeochemical and environmental factors in Fe biomineralization: magnetite and siderite formation. *Clays and Clay Minerals* **51**, 83–95.

Roh Y, Gao H, Vali H, Kennedy DW, Yang ZK, Gao W, Dohnalkova AC, Stapleton RD, Moon J-W, Phelps TJ, Fredrickson JK, Zhou J (2006) Metal reduction and iron biomineralization by a psychrotolerant Fe(III)-reducing bacterium, *Shewanella* sp. Strain PV-4. *Applied and Environmental Microbiology* **72**, 3236–3244.

Sarda C, Mathieu F, Vajpei AC, Rousset A (1987) Size- and surface-dependence of enthalpy of oxidation of submicronic magnetites. *Journal of Thermal Analysis* **32**, 865–971.

Sawiki JA, Brown DA (1998) Investigation of microbial-mineral interactions by Mössbauer spectroscopy. *Hyperfine Interactions* **117**, 371–382.

Shannon D (1976) Revised effective ionic radii and systematic studies of interatomic distances in halides and chalcogenides. *Acta Crystallographica* **A32**, 751–767.

Smirnov AV, Tarduno JA (2000) Low-temperature magnetic properties of pelagic sediments (Ocean Drilling Program Site 805C): tracers of maghemitization and magnetic mineral reduction. *Journal of Geophysical Research* **105**, 16457–16471.

Snowball IF (1993) Geochemical control of magnetite dissolution in subarctic lake sediments and the implication for environmental magnetism. *Journal of Quaternary Science* **8**, 339–346.

Sparks NHC, Mann S, Bazylinski DA, Lovley DR, Jannasch HW, Frankel RB (1990) Structure and morphology of magnetite anaerobically produced by a marine magnetotactic bacteria and a dissimilatory iron-reducing bacterium. *Earth and Planetary Science Letters* **98**, 14–22.

Stapleton RD Jr, Sabree ZL, Palumbo AV, Moyer CL, Devol AH, Roh Y, Zhou J (2005) Metal reduction at cold temperatures by *Shewanella* isolates from various marine environments. *Aquatic Microbial Ecology* **38**, 81–91.

Tamaura Y, Tabata M (1990) Complete reduction of carbon dioxide to carbon using cation-excess magnetite. *Nature* **346**, 255–256.

Tang J, Myers M, Bosnick KA, Brus LE (2003) Magnetite Fe_3O_4 nanoparticles: spectroscopic observation of aqueous oxidation kinetics. *Journal of Physical Chemistry* **B107**, 7501–7506.

Tarduno JA (1995) Superparamagnetism and reduction diagenesis in pelagic sediments: enhanced or depletion? *Geophysical Research Letters* **22**, 1337–1340.

To TB, Nordstrom DK, Cunningham KM, Ball JW, McCleskey RB (1999) New method for the direct determination of dissolved Fe(III) concentration in acid min water. *Environmental Science and Technology* **33**, 807–813.

Vali H, Weiss B, Li Y-L, Sears SK, Kim SS, Kirschvink JL, Zhang CL (2004) Formation of tabular single domain magnetite induced by *Geobacter metallireducens* GS-15. *Proceedings of the National Academy of Sciences, USA* **101**, 16121–16126.

Voogt FC, Fujii T, Smulders PJM, Niesen L, James MA, Hibma T (1999) NO_2-assisted molecular-beam epitaxy of Fe_3O_4, $Fe_{3-\delta}O_4$, and γ-Fe_2O_3 thin films on MgO (001). *Physical Review* **B60**, 11193–11206.

Wagner ID, Wiegel J (2008) Diversity of thermophilic anaerobes. Incredible anaerobes: from physiology to genomics to fuels. *Annals of the New York Academy of Sciences* **1125**, 1–43.

Wiegel J, Ljungdahl LG (1981) *Thermoanaerobacter ethanolicus* gen-nov, spec-nov, a new, extreme thermophilic, anaerobic bacterium. *Archives of Microbiology* **128**, 343–348.

Zachara JM, Kukkadapu R, Fredrickson JK, Gorby YA, Smith SC (2002) Biomineralization of poorly crystalline Fe(III) oxides by dissimilatory metal reducing bacteria (DMRB). *Geomicrobiology Journal* **19**, 179–207.

Zhang Z, Satpathy S (1991) Electron states, magnetism, and the Verwey transition in magnetite. *Physical Review* **B44**, 13319–13331.

Zhang CL, Vali H, Romanek CS, Phelps TJ, Liu SV (1998) Formation of single-domain magnetite by a thermophilic bacterium. *American Mineralogist* **83**, 1409–1418.

Zhang C-L, Li S, Wang L-J, Wu T-H, Peng S-Y (2000) Studies on the decomposition of carbon dioxide into carbon with oxygen-deficient magnetite. I. preparation, characterization of magnetite, and its activity of decomposing carbon dioxide. *Material Chemistry and Physics* **62**, 44–51.